Early Detection of Nitrogen Deficiency in Corn Using High Resolution Remote Sensing and Computer Vision

Dimitris Zermas[1], Panagiotis Stanitsas[1], Daniel Kaiser[2], Vassilios Morellas[1], David Mulla[2] and Nikolaos Papanikolopoulos[1]

[1]Department of Computer Science and Engineering, University of Minnesota, Minneapolis MN

[2]Department of Soil, Water and Climate, University of Minnesota, St. Paul MN

A paper from the Proceedings of the
13th International Conference on Precision Agriculture
July 31 – August 4, 2016
St. Louis, Missouri, USA

Abstract. *The continuously growing need for increasing the production of food and reducing the degradation of water supplies, has led to the development of several precision agriculture systems over the past decade so as to meet the needs of modern societies. The present study describes a methodology for the detection and characterization of Nitrogen (N) deficiencies in corn fields. Current methods of field surveillance are either completed manually or with the assistance of satellite imaging, which offer infrequent and costly information to the farmers about the state of their fields. The proposed methodology promotes the use of small-scale Unmanned Aerial Vehicles (UAVs) and Computer Vision algorithms that operate with information in the visual (RGB) spectrum. Through this implementation, a lower cost solution for identifying N deficiencies is promoted. We provide extensive results on the use of commercial RGB sensors for delivering the essential information to farmers regarding the condition of their field, targeting the reduction of N fertilizers and the increase of the crop performance. Data is first collected by a UAV that hovers over a stressed area and collects high resolution RGB images at a low altitude. A recommendation algorithm identifies potential segments of the images that are candidates exhibiting N deficiency. Based on the feedback from experts in the area a training set is constructed utilizing the initial suggestions of the recommendation algorithm. Supervised learning methods are then used to characterize crop leaves that exhibit signs of N deficiency. The performance of 84.2% strongly supports the potential of this scheme to identify N-deficient leaves even in the case of images where the unhealthy leaves are heavily occluded by other healthy or stressed leaves.*

Keywords. *Remote sensing, nitrogen deficiency, maize, corn, UAV, crop surveillance, drone, computer vision, image analysis, machine learning.*

Introduction

Corn products are used in the everyday life of millions of people around the globe. The wide range of products including feed for livestock, ethanol fuel and various edible products, advocate to the corn's significant value in the world economy. Considering this fact, it is immediately understood that any loss of parts of the corn production due to deficiencies should be prevented.

Existing methods suggest minimizing the expected loss by applying the fertilizers to the corn field several months prior to the cultivation process. These approaches overestimate the amount of fertilizer needed while they increase the counter-effects to the ecosystem; several fertilizer substances dissolve in the ground and end up polluting water sources.

One of the most common and severe deficiencies that farmers need to address relates to the levels of nitrogen the plants have access to. The above statement explains why over the years, many studies (Quemada2014, Blackmer1996) concentrate in N deficiency and treatment. Unfortunately, most of the sensors and methods discussed require human surveillance, which is time consuming and costly. In addition, modern methods of field surveillance that use UAVs limit their applications to high altitude surveillance resulting in solutions that primarily consist of stitched field images which are enriched with statistics based on the fluctuation of the intensity values in the near infrared (NIR) spectra throughout the field.

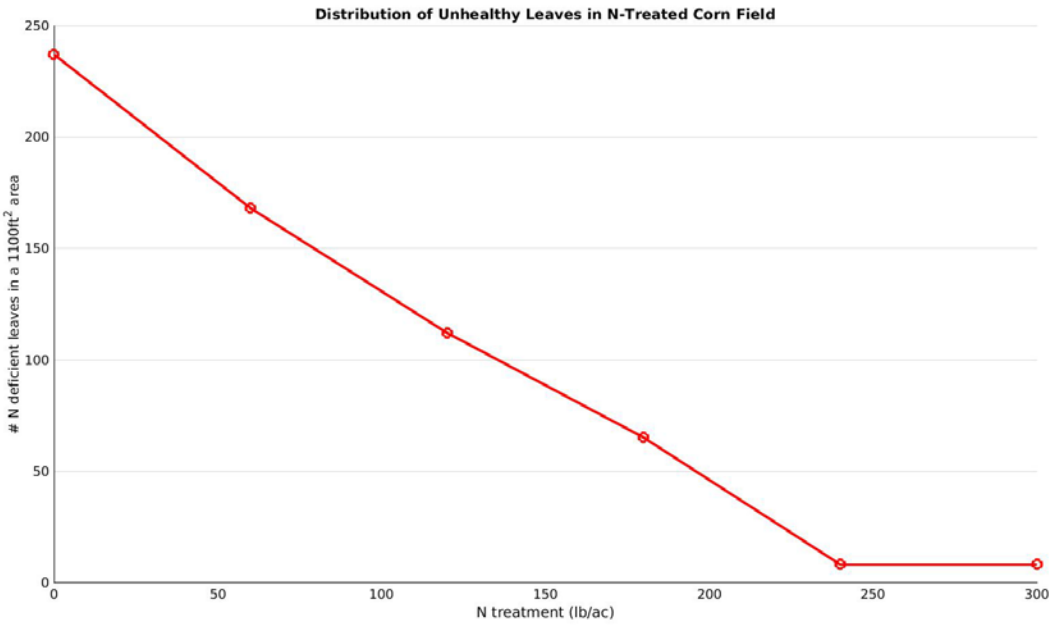

Fig 1. This diagram shows the distribution of the number of N-deficient leaves counted versus the amount of N fertilizer the land received before the seeding process.

To minimize the negative environmental effects of agriculture processes it is vital to optimize the application of fertilizers. This goal requires a system that suggests the amount of fertilizer needed based on a frequent estimation of the deficiencies. Our experiments have shown a clear correlation of the number of N-deficient leaves with the fertilizer that has been applied before the seeding of the plants (Fig. 1). This result reveals the need of an accurate method to estimate the number of deficient leaves.

The main contributions of this work in the field of precision agriculture are summarized as follows:

- Development of a segmentation scheme for robust and accurate clustering of pixels based on color, and
- Introduction of a methodology for the extraction of descriptors that capture N deficiency in corn leaves.

This paper is the first step towards a comprehensive solution for the frequent and low cost surveillance of a corn field and the accurate estimation of the amount of N deficiency in the field.

The remaining sections of this paper are organized as follows. Section II presents a review of the literature regarding the application of computer vision and UAVs to precision agriculture. Section III, discusses an overview of the proposed methodology. A deficient segment recommendation algorithm suggests which parts of the image hold information that could be exploited for the identification of N deficiencies. Then, a supervised module that captures spatial characteristics of leaves in these suggested areas, characterizes them as being N-deficient or not. The presentation of the hardware used is also part of this section. A detailed analysis of the machine learning and computer vision techniques is given in Section IV. Finally, experimental results are presented in Section V, followed by the conclusions and a discussion of future work in Section VI.

Literature Review

The problem of detecting N deficiencies in a corn field has been of great importance amongst corn growers and scientific groups that focus on soil development and plant growth research. Research in the area of remote sensing has introduced several solutions to the problem of nutrient deficiency detection and prevention varying from invasive techniques such as soil and plant sampling, to non-invasive visual inspection over different spectra.

The discussed approaches involve light sensors with sensitivity to various wavelengths and can be classified in the following three categories:

- Visible spectrum imaging,
- Infrared spectrum imaging, and
- Fluorescence excitation.

Mulla et al. (Mulla2013), summarized the significant findings that remote sensing has produced over the last few decades.

The methodologies that dominate the first category utilize satellite and airplane imaging (Quemada2014, Kyveryga2011). Both approaches have the ability to indicate the condition of their fields, but can become costly for cases that a high frequency sampling strategy is required. The shortcomings of these methods have been alleviated with the introduction of small-scale UAVs in the area of precision agriculture.

Rotorcrafts and fixed wing UAVs have recently gained popularity in many areas, especially in agriculture, due to low cost, easy deployment and operational flexibility in visual data collection (Lelong2008, Lucieer2010). Particularly, research work that includes a close up inspection of the plants is limited due to robustness limitations produced by RGB images that are highly dependent on the prevailing lighting conditions.

Research work performed in the thermal and NIR parts of the spectrum offer additional advantages. In particular, work reported in (Osborne2002) shows that NIR data processing is best suited for N deficiency detection. Furthermore, Blackmer et al. (Blackmer1996) published one of the seminal pieces of work that supports the advantages of N deficiency detection in the NIR range.

The advantages of data collection in non visible spectra extend to the spectrum provided by fluorescence imaging. Fluorescence excitation sensors function both as emitters and receivers of

light beams in different spectra. They emit a specific range of spectra, usually in the ultraviolet region and receive the reflected beams. This type of sensing succeeds in providing accurate information on the amounts of nutrients in a plant, by considering a combination of the energy absorbed and the wavelength of the light beam received back from the plant.

The reader can find a review of the fluorescent techniques in the work published by Tremblay et al. (Tremblay2012). Numerous publications consider this approach for nutrient deficiency detection (Quemada2014, Longchamps2014, Malenovsky2009).

Finally, Chaerle et al. (Chaerle2009) collectively present a review on all three categories as well as some attempts to combine different sensors in order to get the most informative outcome. The same group is combining thermal and fluorescence imaging to augment their detection results (Chaerle2007). In addition, (Leinonen2004) combines visible spectrum imagery for the segmentation of plants with a thermal camera for the classification of the plant leaves. In this last publication, the visual spectrum is utilized as an assisting tool for leaf segmentation, in contrast to the current work which treats it as the main element in the deficiency detection pipeline.

The goal of this work is to develop a monitoring system for corn plants that is automated, effective, and low cost. The effectiveness of the infrared spectra as well as the fluorescent excitation methods is evident in the aforementioned publications, but the utilization of such sensors seems incompatible with the low cost and light payload constraints imposed by a small-scale robotic framework. This realization suggests that a solution should be sought in the direction of the visible spectrum sensors, where the hardware shortcomings should be confronted by shifting the efforts towards the development of more sophisticated software.

Architecture

Architecture Overview

Our approach heavily relies on the collection of visible images. High resolution RGB images are initially collected by a small-scale UAV at a low altitude flight (15-25m) and covers an area of the field that exhibits evidence of stress. The flight is semi-automated with waypoints provided beforehand and the camera is manually triggered once the UAV reaches a waypoint.

A visual observation reveals certain image characteristics that guide the proposed methodology for detecting N deficiency. As seen in Fig. 2, the proposed methodology capitalizes on two features: (i) the unhealthy part is denoted by the yellow colored part of the leaf, and (ii) the “V” shape outlined by the complement of the yellow component of the leaf with respect to its healthy (green) counterpart.

Fig 2. Samples of healthy (top) and N-deficient (bottom) leaves.

The two aforementioned characteristics are directly associated with the two implementation modules we developed. The first module results in locating the areas in the form of rectangular regions

exhibiting potential N deficiency. The second module acts as a filter of the output of the first module, further refining the decision of correctly identifying leaf areas of N deficiency with high degree of confidence.

Hardware

The data collection process is aided by the deployment of a small-scale UAV robot with an attached high resolution RGB camera. The robotic platform, which is a MikroKopter Okto XL (Fig. 3), has the ability to carry a payload of 2500g and when loaded with the sensor has a flight time of 15 minutes. The embedded RGB camera is a Nikon D7100 weighs 675g, and has the ability to capture images up to 4000 x 6000 resolution.

Fig 3. A RGB camera mounted on the robotic platform Mikrokopter Okto XL.

This apparatus allows the user to inspect the sensor's feedback via a Wi-Fi transmitter which is mounted on the UAV and streams low quality video to a video screen, supporting precise image capturing.

Algorithmic Components

In this section, the two data processing modules are discussed in detail starting with the first module (recommendation scheme) followed by the second module (N deficiency assessment).

Recommendation Scheme

The first step towards identifying N-deficient leaves in images is to recommend image regions that hold significant information regarding the general state of health of the individual leaves. This is an important step in the process pipeline, because it limits the computations to only small image areas, thus increasing performance and reducing computational time.

The concept behind a recommendation algorithm is the selection of meaningful subsets of pixels from a given image and this work identifies such subsets following the exhibited homogeneity of their color spaces. The conceptual flow of this recommendation module can be found in Fig. 4.

Pixels are clustered based on color and the goal is to partition them in 3 clusters. The first cluster consists of green pixels, the second of yellow pixels (associated with potential N deficiencies), and the last of pixels that correspond to the soil. The experimentation with the pixels' distribution in several color spaces has indicated that using an unsupervised clustering algorithm tends to naturally separate green pixels from the other dominant colors, namely yellow and brown. Following the

aforementioned observation, this algorithm initially aims to segment only the green pixels of the image by employing a hierarchical K-means algorithm (Jain1999) and combining the clustering results of two color spaces; RGB and L*a*b (Jain1989).

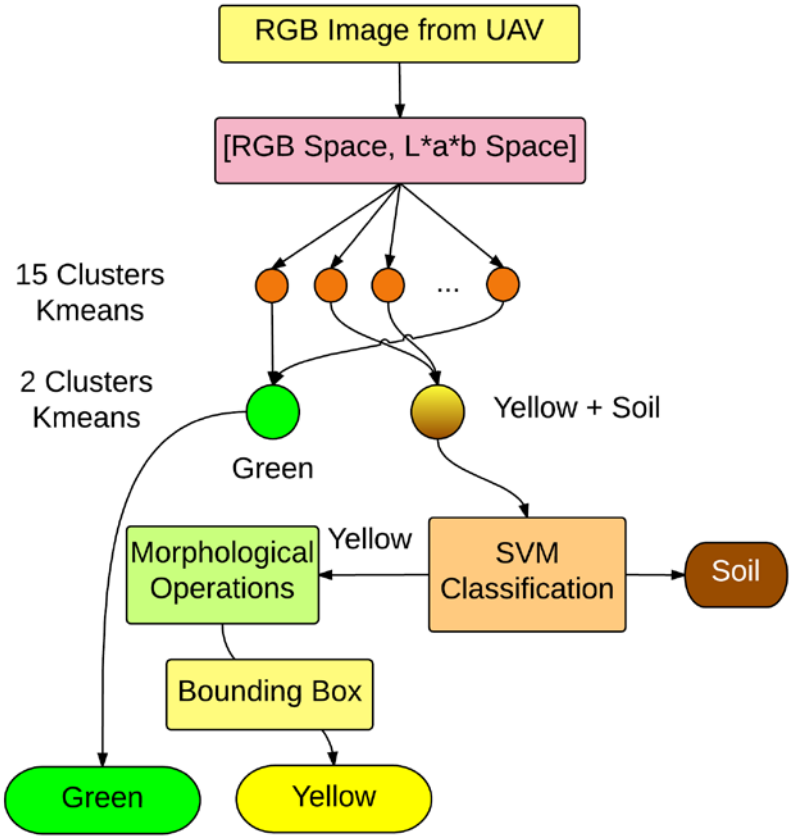

Fig 4. The flow chart visualizes the steps followed by the recommendation scheme.

The unsupervised clustering implementation in each color space concludes in two steps starting with a 15-class clustering that breaks down the image into groups of similar colored pixels, and finishing with a 2-class clustering that separates the green clusters from the combination of yellow and soil clusters.

The initialization of K-means is random for the first clustering that involves thousands of pixels, but is biased in the second step where only 15 queries are clustered. The bias is introduced in both color spaces by selecting a green initialization point from a normal distribution with its mean deep into the green region.

The naive approach of segmenting the green parts in a single color space is not accurate for all images. This is especially true in cases with a few N deficiencies, where a significant variance in the representation of the green color is present. The accuracy of the segmentation increases when combining the clustering results of the two color spaces. This method achieves robust results in the segmentation of green pixels for all the subject images.

When dealing with the NIR spectra, the concept of the soil line (Baret1993) is widely used and provides an accurate index for the identification of the soil pixels. On the other hand, in the visible spectrum the automated distinction between yellow pixels and pixels belonging to the soil proves to be particularly challenging.

Once green pixels are separated from the rest, a semi-supervised classification scheme partitions the non-green pixels into yellow and soil clusters. The process developed asks the user to draw a single rectangle around pixels that represent soil and another rectangle around yellow pixels which represent leaves with N deficiency. Consecutively, an SVM classification model with a linear kernel is trained based on these selections and is used for the classification between yellow and soil in the rest of the images. Finally, connected regions of yellow pixels are smoothed by morphological operators and bounding boxes are assigned to them in an effort to highlight informative candidate regions.

Specifically, parts of the plant that are one pixel apart are connected in order to remove discontinuities while morphological opening and closing are used as hole filling techniques for the removal of empty patches inside the hull of the leaves. The smooth and symmetrical objects that result from these morphological operations guarantee high performance of the feature extraction step described in the next section.

An additional morphological step removes small groups of pixels based on a threshold that considers their size. The threshold is manually selected through a trial and error process and can fluctuate depending on the resolution of the initial image. The surviving groups are the candidates for the second module (Fig. 5).

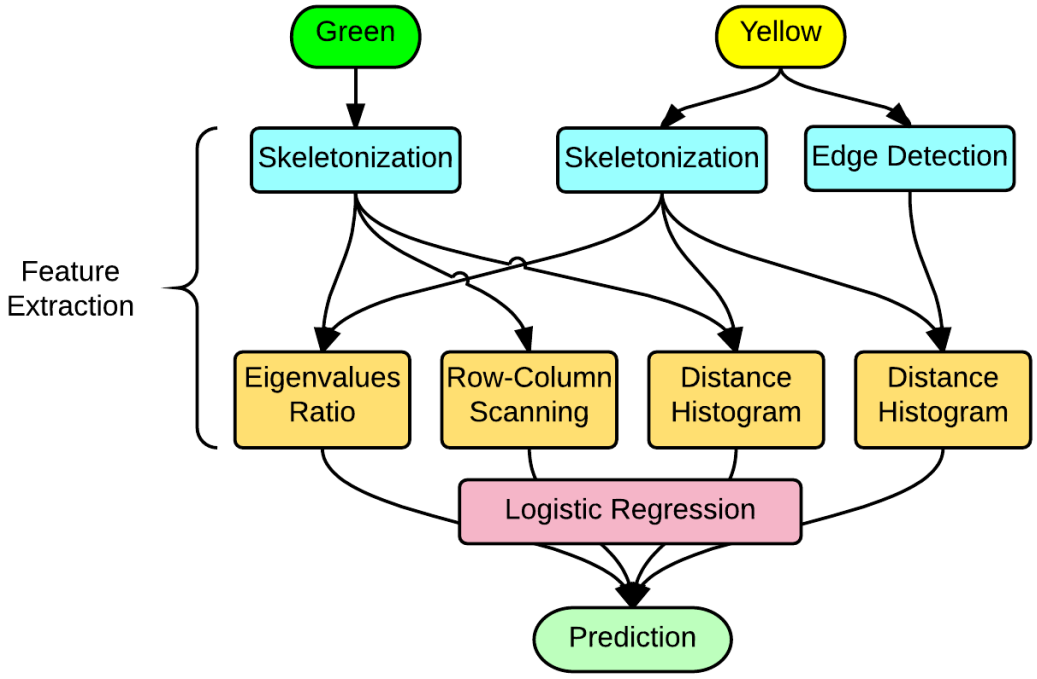

Fig 5. The flow chart presents the steps that lead to the N deficiencies assessment of an image.

Deficiency Assessment

In this step, an assessment regarding the deficiency of a candidate region is performed. The inputs consist of rectangular regions suggested by the recommendation algorithm, and depict potentially affected parts of the image. Among the selected candidates, the leaves that are exhibiting N deficiency need to be separated from the rest (e.g. tassels or stressed leaves for which assessment

cannot be made).

This distinction is based on the "V" shaped deformation that is directly associated with the N deficiency. A skeletonization algorithm (Telea2002), based on the contrast of the yellow and green pixels in the suggested rectangular regions, is responsible for constructing spatial descriptions of this deformation. The extracted descriptors are then used to train a classification model, which in turn makes an assessment on the existence of N deficiencies in the suggested region. The extrapolation of the spatial features needs to take into account that the orientation of the leaves as well as their size depend on the position of the camera and the growth of the plant, and thus the extracted features need to be scale and rotation invariant.

In addition to the skeletonization algorithm, an edge detection algorithm based on gradients is deployed. Features are extracted using skeletons and edges of the green and yellow areas in the segmented regions as derived from the recommendation algorithm. The coordinates of the pixels belonging to skeletons and edges are normalized with respect to the size of their respective bounding box, in order to introduce scale invariance in the methodology.

First, the covariance matrices of the green and yellow skeletons are extracted and their eigenvalues are computed. In this case, the covariance matrix $C \in R^{2x2}$describes the distribution of the pixels of the skeleton around its centroid. Its two eigenvalues σ_1, $\sigma_2$capture the dispersion of the pixels along the direction of the two eigenvectors of C. The ratio of the two eigenvalues $\sigma_2/\sigma_1$is a feature that encapsulates the shape of the skeleton.

Next, the spatial relation between the yellow segment's skeleton and edges is captured by a histogram of the minimum distances between points of the skeleton and the edges. This approach ensures the rotation invariance of the features and is repeated to compute a histogram between the skeletons of green and yellow segments. Particularly, the histogram of minimum distances is computed as follows.

The distance vector $d \in R^{n_s}$, where $n_s$is the number of pixels of the skeleton, is calculated as:

$$d_i = min\left|\left|s_i - e_j\right|\right|, \forall j = 1,\ldots,n_c \; and \; i = 1,\ldots,n_s, \quad (1)$$

where s_i are the pixels of the skeleton, e_j are the pixels of the edges and n_e is the number of pixels of the edges.

This approach can be generalized to capture the spatial relation of any two line segments. If the histogram of distances is seen as a distribution of points, then the features that characterize it are the first four moments of this distribution: (i) the mean, (ii) the variance, (iii) the skewness, and (iv) the kurtosis.

Finally, the recommended segments are scanned vertically and horizontally counting how many times the skeleton of the green part is encountered in each row and column.

As presented in Fig. 6, for a N-deficient leaf, the distribution of the skeletons tends to be elongated towards one direction, the distances between the skeleton and edges that the methodology considers are distributed symmetrically around the yellow part's skeleton in an almost consistent distance, and the skeleton of the green part that is enclosing the yellow part is encountered two times during the rows' and columns' scanning.

On the other hand, non-N-deficient suggestions generally have a cyclic distribution of skeletons, the distances between skeletons and edges are irregular, and in the case of tassels the scanning process would encounter the same skeleton multiple times.

Based on the feature space created, a Logistic Regression classifier is trained and then used for classification purposes. Logistic Regression is selected over Naive Bayes and SVM with linear kernels, because it achieves a better overall accuracy. As shown later in the experimental results, the

imbalance in the number of queries between the two classes of the classification introduces problems regarding the sensitivity of the model for the Logistic Regression classifier. Sacrificing the accuracy for a better balance between sensitivity and specificity can be achieved through an SVM classifier with RBF kernels.

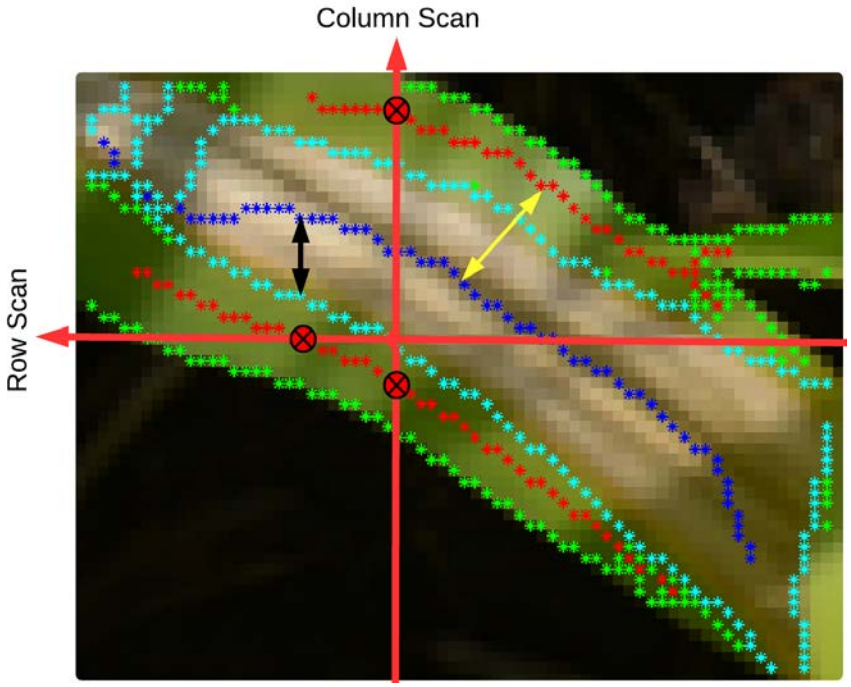

Fig 6. This figure assists with the visualization of the features extracted for the prediction of N-deficient leaves. The green and cyan asterisks show the edges of green and yellow areas respectively, while red and blue are their skeletons. The yellow arrow presents an example of a pair of point between green and yellow skeletons with the minimum distance, and the black arrow is a sample minimum distance of the skeleton-edge pair for the yellow part. The vertical and horizontal red arrows simulate the scanning process and the red crosses found on them are the successful matches of the green part's skeleton.

Experimental Results

Prior to the presentation of the results, it is important to address a major obstacle when dealing with the visible spectrum imaging, which is the illumination inconsistency. The application of the proposed scheme to a real world setting requires the assembly of information regarding the weather conditions during the flight. The findings based on the National Climatic Data Center of the National Oceanic and Atmospheric Administration (NOAA) show that 30% of the days of the year that corn is being grown the sunshine provides ideal illumination for imaging, while about 60% of the same period of time the existing weather conditions advocate for an acceptable analysis of RGB images. These findings suggest that the proposed architecture is capable of providing information throughout the biggest portion of the corn growing cycle.

The dataset spans over a range of six different N fertilizer concentrations (0, 60, 120, 180, 240, 300lbs/ac), four plant growth stages (V6, V8, V10, V12) and two different soil varieties (sandy, compost). It consists of high resolution RGB images gathered by the MikroKopter Okto XL (Fig. 3). All plants were planted the same day and the soil differences in nutrients and color are statistically insignificant. The data collected by the UAV were transferred to a remote station that handled the offline computations upon the completion of the flight.

Recommendation Scheme

The first step of the proposed architecture includes the validation of the accuracy of the segmentation

algorithms as well as the performance of the recommendation scheme. The results for the green pixels' segmentation are summarized in Table 1. These results were computed with the help of 4 hand-drawn masks (2 for each case of severe and light deficiency) created on 4 different images.

Table 1. Green pixels' segmentation accuracy in different color spaces

Deficiency level	RGB	L*a*b	Combined Spaces
Heavy	96.0%	97.0%	96.4%
Light	70.2%	51.7%	92.3%

It is evident from the last column of Table 1 that the mixed spaces hierarchical K-means scheme performs better than a naive single color space K-means approach, since it remains consistently accurate for the different levels of N deficiency (heavy and light). In Figures 7.a and 7.b, the results of the segmentation on a heavily deficient and lightly deficient image are shown.

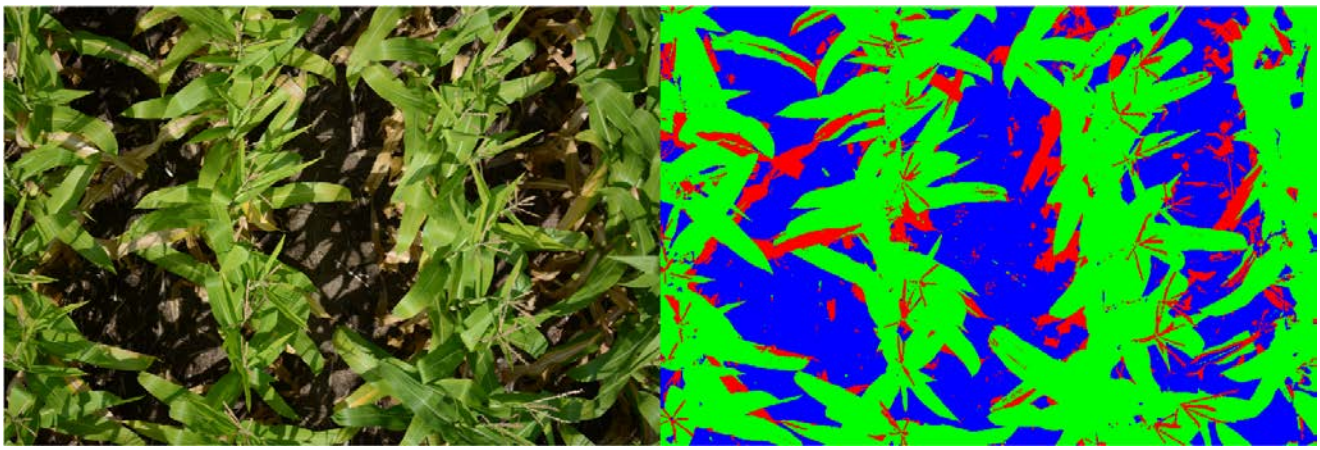

Fig 7.a. The results of the segmentation steps of a heavily N-deficient image. The clusters on the right are: green - green pixels, red - yellow pixels, blue - soil pixels.

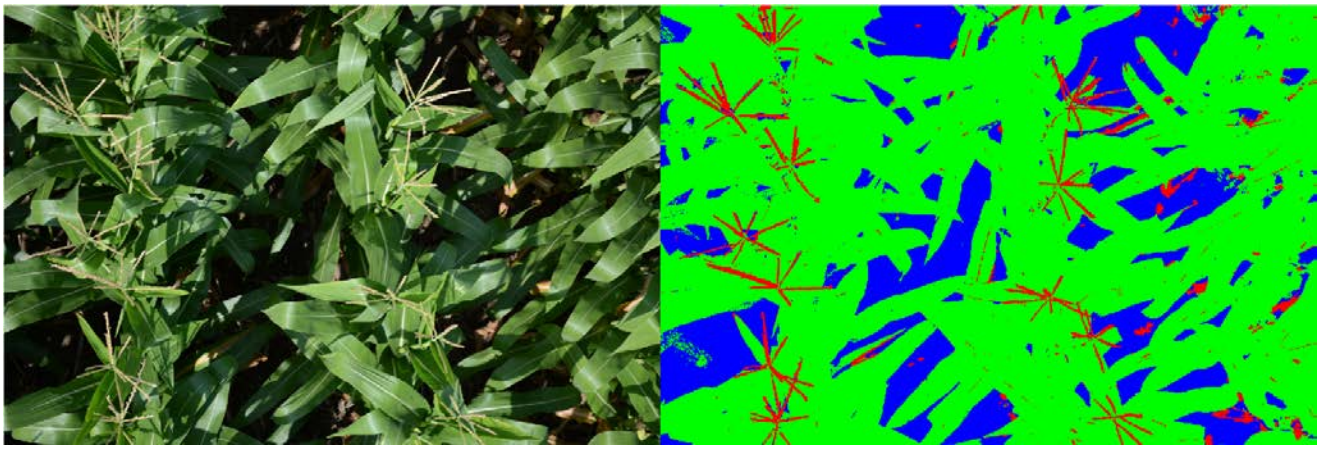

Fig 7.b. The results of the segmentation steps of a lightly N-deficient image. The variance of the green color can be seen in the left half of the image. The clusters on the right are: green - green pixels, red - yellow pixels, blue - soil pixels.

Applying the recommendation algorithm on all the captured images resulted in the creation of over nine thousand (9,000) queries including N-deficient leaves, tassels, and non-N-deficient yellow regions. Around three thousand (3,000) of the queries were groundtruthed as N-deficient, while the

remaining six thousand (6,000) were assessed as being non-N-deficient. The percentage of N-deficient leaves that were missed during the suggestion phase was manually estimated at 5.3% for the severely deficient case and 23.1% for the images with the healthier plants. The undetected areas in the second case are due to the heavy occlusion and the absence of illumination in the lower leaves of the plants making their discernment challenging even for a human. This outcome does not undermine the value of the proposed methodology, since it applies to plants whose yield is not significantly affected by the lack of N.

N Deficiency Assessment

The classification models were trained on a subset of the total number of queries and applied to a test set to measure the performance of the method following a 10-fold validation scheme. The classification of N-deficient leaves versus the rest non-N-deficient suggestions for a Logistic Regression classifier achieved 84.2% correct classification for heavily deficient cases (0, 60, 120lb/ac) and 72.9% for the light deficient cases (180, 240, 300lb/ac). In the second case, several suggestions that represent tassels and sun reflections on the healthy leaves were falsely assigned as N-deficient resulting in a drop of performance when compared to the first case. Combining both cases, an overall 79.2% accuracy was reached, with the specificity and sensitivity of the Logistic Regression model being 95% and 29.5% respectively.

The high specificity percentage shows that the algorithm is particularly capable of detecting suggestions that are truly non-N-deficient, while the sensitivity result suggests that it lacks the ability to robustly identify the true N-deficient leaves. The two-to-one ratio between the number of queries of the two classes (6,000 to 3,000) is an important factor that relates directly to the performance of the Logistic Regression. Essentially, this ratio favors the selection of more samples from the non-N-deficient queries during the training process, biasing the final parameter estimation of the classifier.

As suggested earlier, it is possible to achieve a better balance between specificity and sensitivity by utilizing a SVM classifier with RBF kernels. Table 2 presents the accuracy, sensitivity, and specificity for the Logistic Regression versus SVM classifiers with several sigma parameters. These results show that it is possible to attain a better sensitivity outcome with the sacrifice of accuracy. Depending on the desired outcome of the application, different classification models may be used. For example, it is possible to use the Logistic Regression approach to robustly identify the leaves that are not N-deficient and redirect the attention of the farmer to a smaller number of leaves that are more probable to exhibit N deficiency. On the other hand, exploiting the SVM with RBF kernel models can achieve a balanced classification outcome able to successfully suggest true N-deficient leaves.

Table 2. Accuracy, Sensitivity, and specificity for Logistic Regression (LR) and SVM with RBF kernels (SVM) of different σ parameters.

	LR	SVM ($\sigma = 1$)	SVM ($\sigma = 2$)	SVM ($\sigma = 4$)	SVM ($\sigma = 6$)	SVM ($\sigma = 8$)
Accuracy	79.2%	74.4%	73.7%	72.3%	70.8%	68.9%
Sensitivity	29.5%	19.3%	55.0%	62.1%	61.8%	62.7%
Specificity	95.0%	94.2%	80.4%	76.0%	74.0%	71.1%

Although the images were collected in different altitudes, the algorithm shows robustness and is able to pinpoint N deficient leaves in different resolutions. This property is particularly interesting in cases where the camera has not advanced zooming capabilities, or when the UAV is constrained in flying over a certain height.

The following images depict detected N deficient leaves in the several corn deficient cases we considered. During the early stages of the plant growth and especially in compost soil, the deficiencies are rarely visible therefore no results are shown. Particularly, stages V6, V8, and V10 (Figures 8.a and 8.b) only show deficiencies for the sandy soil when no fertilizer was applied. The

plants growing in the compost soil, seem to absorb nutrients from the soil itself and do not exhibit yellowness on their leaves. Furthermore, the treatments of 240 and 300lbs/ac seem to not presenting any significant deficiencies no matter the stage or soil conditions. The cases presented in Figures 9.a-e, present the results of our algorithm in sample cases of plants in their V12 growth stage and for different N treatment (0, 60, 120, 180, 240lbs/ac).

Fig 8.a. Detection of N deficient leaves at stage growth V6. Deficiency visible only on plants that were not treated with N fertilizer.

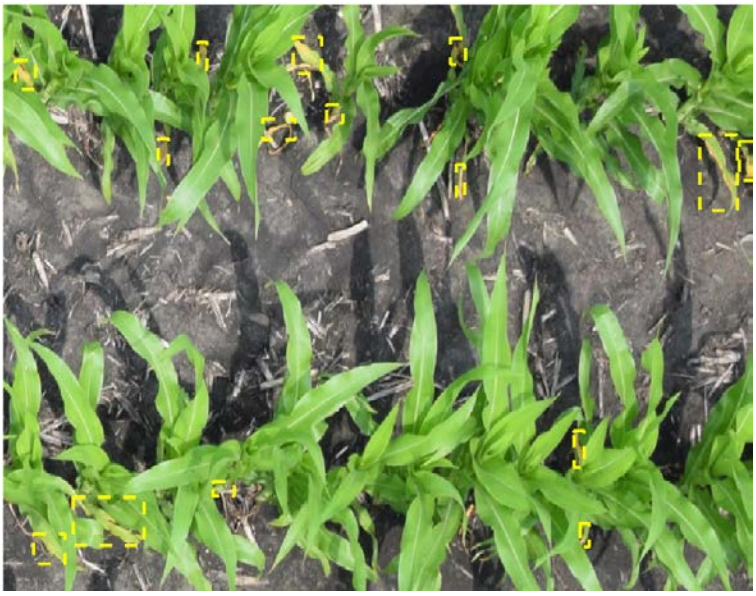

Fig 8.b. Detection of N deficient leaves at stage growth V10. Deficiency visible only on plants that were not treated with N fertilizer.

Fig 9.a. Detection of N deficient leaves at stage growth V12. The plants have received no N treatment.

Fig 9.b. Detection of N deficient leaves at stage growth V12. The plants have received 60lbs/ac N treatment.

Fig 9.c. Detection of N deficient leaves at stage growth V12. The plants have received 120lbs/ac N treatment.

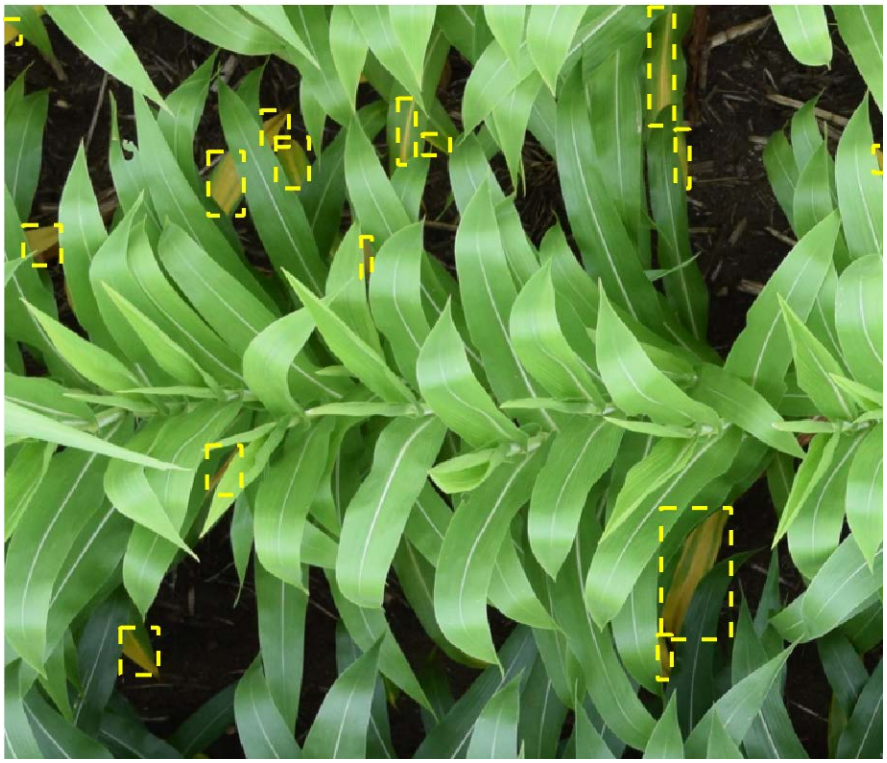

Fig 9.d. Detection of N deficient leaves at stage growth V12. The plants have received 180lbs/ac N treatment.

Fig 9.e. Detection of N deficient leaves at stage growth V12. The plants have received 240lbs/ac N treatment.

Conclusion and Future Work

The current work serves as a proof of concept for an architecture that brings forth a new perspective in field monitoring. UAVs can be utilized along with inexpensive RGB camera sensors to enable the acquisition of a more detailed view of the field's condition. The results of the proposed methodology support the choice of using ordinary images in the visible spectrum, taken by a sensor that has significantly lower cost than its rivals that operate in the invisible spectrum.

A performance of 84.2% is achieved for the correct classification between N-deficient leaves and non-N-deficient yellow image segments. This result sets a strong basis for more elaborated attempts towards the utilization of RGB imaging for close up precision agriculture in fields. The use of UAVs is a major asset in precision agriculture, but is currently not fully utilized. Hopefully, the attempts to bridge flying robots with farm automation will prove to be fruitful in the near future as this architecture matures. A significant addition to the current work will be the complete automation of the flight of the robot including its path planning and data gathering.

The current study has examined a range of cases of N-deficient corn plants that have received different N treatment and were cultivated in two different types of soil. Additional data that cover N deficiency levels in more soil types is going to allow the direct correlation of the number of deficient leaves detected with the N levels in the soil. This addition could assist the estimation of the amounts of fertilizers to be purchased and applied, and would expand the capabilities of the proposed approach resulting in an architecture that is directly applicable to real world situations.

Acknowledgements

This work was carried out in part using support from the Minnesota Corn Research and Promotion Council. This material is also based upon work supported by the National Science Foundation through grants #IIP-0934327, #IIP-1032018, #IIS-1017344, #CNS-1061489, #CNS-1138020, #IIP-1127938, #IIP-1237259, #IIP-1332133, #IIS-1427014, #IIP-1432957, and #CNS-1531330.

References

Baret, F., Jacquemoud, S., and Hanocq, J.F., "The soil line concept in remote sensing," Remote Sensing Reviews, vol. 7, no. 1, pp. 65–82,1993.

Blackmer, T., Schepers, J., Varvel, G., and Walter-Shea, E., "Nitrogen deficiency detection using reflected shortwave radiation from irrigated corn canopies," Agronomy Journal, vol. 88, no. 1, pp. 1–5, 1996.

Chaerle, L., Lenk, S., Leinonen, I., Jones, H.G., Van Der Straeten, D., and Buschmann, C., "Multi-sensor plant imaging: Towards the development of a stress-catalogue," Biotechnology Journal, vol. 4, no. 8, pp. 1152–1167, 2009.

Chaerle, L., Leinonen, I., Jones, H.G., and Van Der Straeten, D., "Monitoring and screening plant populations with combined thermal and chlorophyll fluorescence imaging," Journal of Experimental Botany, vol. 58, no. 4, pp. 773–784, 2007.

Jain, A.K., Murty, M.N., and Flynn, P.J., "Data clustering: A review," ACM Comput. Surv., vol. 31, no. 3, pp. 264–323, Sep. 1999.

Jain, A.K., Fundamentals of Digital Image Processing. Upper Saddle River, NJ, USA: Prentice-Hall, Inc., 1989.

Kyveryga, P., Blackmer, T., and Pearson, R., "Normalization of uncalibrated late-season digital aerial imagery for evaluating corn nitrogen status," Precision Agriculture, vol. 13, no. 1, pp. 2–16, 2012.

Leinonen, I., and Jones, H.G., "Combining thermal and visible imagery for estimating canopy temperature and identifying plant stress,"Journal of Experimental Botany, vol. 55, no. 401, pp. 1423–1431, 2004.

Lelong, C.C.D., Burger, P., Jubelin, G., Roux, B., Labbé, S., and Baret, F., "Assessment of unmanned aerial vehicles imagery for quantitative monitoring of wheat crop in small plots," Sensors, vol. 8, no. 5, pp. 3557–3585, 2008.

Longchamps, L., and Khosla, R., "Early detection of nitrogen variability in maize using fluorescence," Agronomy Journal, vol. 106, no. 2, pp. 511–518, 2014.

Lucieer, A., Robinson, S.A., and Turner, D., "Using an unmanned aerial vehicle (UAV) for ultra-high resolution mapping of antarctic moss beds," 15th Australasian Remote Sensing Photogrammetry Conference, 2010.

Malenovský, Z., Mishra, K.B., Zemek, F., Rascher, U., and Nedbal, L. "Scientific and technical challenges in remote sensing of plant canopy reflectance and fluorescence," Journal of Experimental Botany, vol. 60, no. 11, pp. 2987–3004, 2009.

Mulla, D. J., "Twenty five years of remote sensing in precision agriculture: Key advances and remaining knowledge gaps," Biosystems Engineering, vol. 114, no. 4, pp. 358–371, 2013, special issue: Sensing Technologies for Sustainable Agriculture.

Osborne, S.L., Schepers, J.S., Francis, D.D., and Schlemmer, M.R., "Detection of phosphorus and nitrogen deficiencies in corn using spectral radiance measurements," Agronomy Journal, vol. 94, no. 6, pp.1215–1221, 2002.

Quemada, M., Gabriel, J.L., and Zarco-Tejada, P. "Airborne hyper-spectral images and ground-level optical sensors as assessment tools for maize nitrogen fertilization," Remote Sensing, vol. 6, no. 4, pp. 2940–2962, 2014.

Telea, R. and Wijk, J.J.V., "An augmented fast marching method for computing skeletons and centerlines," in Proc. of the Symposium on Data Visualisation (VisSym'02), 2002, pp. 251–259.

Tremblay, N., Wang, Z., and Cerovic, Z.G., "Sensing crop nitrogen status with fluorescence indicators. a review," Agronomy for Sustainable Development, vol. 32, no. 2, pp. 451–464, 2012.